

Effect of aliphatic diacyl adipic dihydrazides on the crystallization of poly(lactic acid)

Zhongfei Qi,^{1,2} Yong Yang,¹ Zhu Xiong,¹ Jun Deng,¹ Ruoyu Zhang,¹ Jin Zhu¹

¹Ningbo Key Laboratory of Polymer Materials, Ningbo Institute of Materials Technology and Engineering, Chinese Academy of Sciences, Ningbo, Zhejiang 315201, People's Republic of China

²School of Natural and Sciences Northwestern Polytechnical University, Xi'an, Shaanxi 710129, People's Republic of China

Correspondence to: J. Zhu (E-mail: jzhu@nimte.ac.cn) and R. Y. Zhang (E-mail: zhangruoyu@nimte.ac.cn)

ABSTRACT: A series of aliphatic diacyl adipic dihydrazides (ADHs) with different alkyl moieties were synthesized by the reaction between adipic dihydrazide and acyl chloride. Then these ADHs were solution blended with PLA respectively and were evaluated as nucleating agents. Through the investigation of nonisothermal and isothermal crystallization, it was found that both the crystallization rate and the crystallinity of PLA could be enhanced by adding only 1 wt % of ADHs. Especially for ADH-Oc (ADH-Octyl), the crystallization rate of PLA increased about 4 times at 105°C. Optical morphology showed that and the size of PLA spherulites decreased and the nucleation density increased with the existence of ADH-Oc. Meanwhile, the crystal structure of PLA were not discernibly affected after the addition of ADHs as found by wide-angle X-ray diffraction. Thus, this study suggested these ADHs compounds are simple and potential nucleating agents to enhance crystallization ability of PLA. © 2015 Wiley Periodicals, Inc. *J. Appl. Polym. Sci.* 2015, 132, 42028.

KEYWORDS: biodegradable; blends; crystallization; synthesis and processing; thermal properties

Received 4 October 2014; accepted 19 January 2015

DOI: 10.1002/app.42028

INTRODUCTION

Poly(lactic acid) (PLA) is one of the most important biocompatible and biodegradable polymers, and the monomers of which are generally produced by fermentation of renewable natural resources like corn and sugar cane, etc.^{1,2} PLA not only can be used in biomedical areas,^{3,4} but also has substituted some conventional plastics and packing materials to a certain extent because of its good mechanical properties.^{5–8} However, the crystallinity of neat PLA is usually very low because of its slow crystallization rate, which leads to a long processing period and poor heat resistance, and limits its extensive applications.^{9,10} Numerous studies have been carried out to improve the crystallization ability of PLA, such as adding nucleating agent,^{11–14} adding plasticizer,^{15–17} and optimizing the molding condition^{18,19} *et al.* However, one of the most useful and effective way is recognized as adding nucleating agent in PLA.

Inorganic and organic nucleating agents had already been used in PLA. Talc, clay, and montmorillonite are common examples of inorganic compounds that had been reported to effectively enhance the crystallization of PLA.^{20–23} But the physical properties of these PLA composites were rather low when adding these

nucleating agent.²¹ Organic compounds can also promote the crystallization rate of PLA. This is typically achieved by adding some low molecular weight substances which will crystallize at temperature higher than the crystallization temperature of PLA and provide nucleation sites. It was reported that adding N,N-ethylenebis (12-hydroxystearamide) (EBH) could tremendously increase the nucleation rate of PLA.²⁴ At high crystallization temperatures, the nucleation density of PLA in the presence of EBH increased 40 times and the overall crystallization rate increased four times. Compared with EBH, another low molecular weight aliphatic amides, N,N'-ethylenebisstearamide (EBSA), also showed effective nucleation ability in PLA because of the hydrogen bond between amide bond and chains of PLA.²⁵ Moreover, the hydrazide group is considered to be a functional group for designing an effective nucleating agent for PLA, such as N,N-bis(benzoyl) alkyl diacid dihydrazides.²⁶ Kawamoto *et al.*^{27,28} compared the nucleating ability of hydrazide compounds with talc and EBH in PLA. It was found that selected hydrazide compounds enabled PLA to complete crystallization upon cooling with a high crystallization enthalpy (ΔH_c) of 46 J/g, while that of Talc and EBH only showed ΔH_c of 26 and 35 J/g under the same conditions, respectively. The

hydrazide compounds, which containing stronger hydrogen bond between nucleating agent and PLA chains, might further enhance crystallization ability of PLA. However, to the best of our knowledge, few literatures reported the investigation of aliphatic hydrazide compounds as nucleating agents in PLA, which could also form strong hydrogen bond with PLA chains.

In this article, a series of aliphatic diacyl adipic dihydrazides (ADHs) with different alkyl moieties were synthesized from adipic dihydrazide and acyl chloride, and were investigated as nucleating agent of PLA. Nonisothermal and isothermal crystallization processes were studied to evaluate the crystallization of neat PLA and PLA/ADHs blends. Morphologies and crystal growth rate were also investigated by polarized optical microscope (POM). Besides, the crystalline structures of PLA/ADHs blends samples were evaluated by wide-angle X-ray diffraction. At last, the nucleation effect of different ADHs were compared and discussed.

EXPERIMENTAL

Materials

PLA (commercial grade 4032D, consist of ~2% D-LA) was purchased from Nature Works LLC. The aliphatic diacyl adipic dihydrazides were synthesized as the procedure listed in the next section. Adipic dihydrazide and acyl chloride were purchased from Aladdin Chemistry (Shanghai, China) and with no further purification. All the other reagents and solvents were obtained from Sinopharm Chemical Reagent and used without further purification.

Synthesis of ADHs

Four ADHs with different alkyl moieties as Hexyl (He), Octyl (Oc), Decyl (De), and Lauryl (La) groups were synthesized in the same experimental procedure. The procedures were operated as follows: 10 mmol adipic dihydrazide was suspended in 30 mL N,N-Dimethylformamide (DMF), added 30 mmol triethylamine used as acid-binding agent, and then dropwise added 25 mmol acyl chloride below 3°C. The mixture was stirred for 30 min at low temperature and then reacted at 50°C for 5 hours. Then the reaction mixture including ADHs was cooled in air to room temperature then poured into cold water with stirring to form insoluble floc. The floc was filtered off and washed with water and alcohol successively for several times, then dried at 80°C in vacuum oven for 12 hours. Finally, white ADHs crystals were collected and characterized by ¹H NMR, Fourier transform infrared (FTIR), and differential scanning calorimetry (DSC).

Characterization

FTIR spectra of ADHs were carried out by a Nicolet 6700 spectrophotometer by use of KBr. The ¹H NMR spectra of ADHs were recorded with a Bruker instrument (400-MHz AVANCE III). The ADHs samples were dissolved in DMSO and tetramethyl silane was used as an internal standard. Melting temperatures (*T_m*) of ADHs were recorded with DSC instrument (Mettler-Toledo, TGA/DSC 1, Switzerland) under nitrogen protection from 25°C to 300°C at a heating rate of 5°C/min. FTIR, ¹H NMR results and *T_m* were listed below. As can be seen from

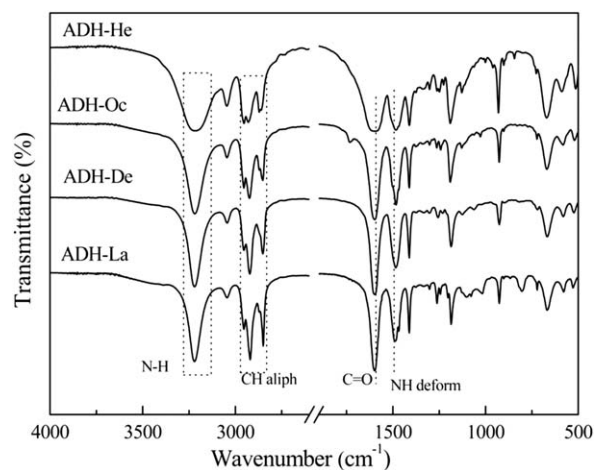


Figure 1. FTIR spectra of different ADHs.

the characterization results in Figures 1 and 2, we have synthesized the ADHs successfully.

ADH-He (C₁₈H₃₄N₄O₄): ¹H NMR (400 MHz DMSO-d₆, δ in ppm): 0.86 (t, 3H, CH₃), 1.25 (m, 2H, CH₂), 1.49 (m, 2H, CH₂), 2.06 (m, 2H, CH₂), 9.64 (s, 1H, N-H); IR (KBr): ν = 3320 (N-H), 2918 and 2846 (C-H aliph), 1604 (C=O), 1481 (N-H deform); *T_m* = 272°C.

ADH-Oc (C₂₂H₄₂N₄O₄): ¹H NMR (400 MHz, DMSO-d₆, δ in ppm): 0.86 (t, 3H, CH₃), 1.25 (s, 2H, CH₂), 1.51 (s, 2H, CH₂), 2.08 (t, 2H, CH₂), 9.64 (s, 1H, N-H); IR (KBr): ν = 3321 (N-H), 2920 and 2845 (C-H aliph), 1605 (C=O), 1481 (N-H deform); *T_m* = 262°C.

ADH-De (C₂₆H₅₀N₄O₄): ¹H NMR (400 MHz, DMSO-d₆, δ in ppm): 0.88 (d, 3H, CH₃), 1.28 (s, 2H, CH₂), 1.41 (d, 2H, CH₂), 2.12 (d, 2H, CH₂), 9.65 (s, 1H, N-H); IR (KBr): ν = 3321 (N-H), 2921 and 2844 (C-H aliph), 1604 (C=O), 1483 (N-H deform); *T_m* = 260°C.

ADH-La (C₃₀H₅₈N₄O₄): ¹H NMR (400 MHz, DMSO-d₆, δ in ppm): 0.83 (d, 3H, CH₃), 1.23 (s, 2H, CH₂), 1.46 (s, 2H, CH₂), 2.00 (m, 2H, CH₂), 9.61 (s, 1H, NH); IR (KBr): ν = 3322 (N-H), 2922 and 2844 (C-H aliph), 1606 (C=O), 1484 (N-H deform); *T_m* = 253°C.

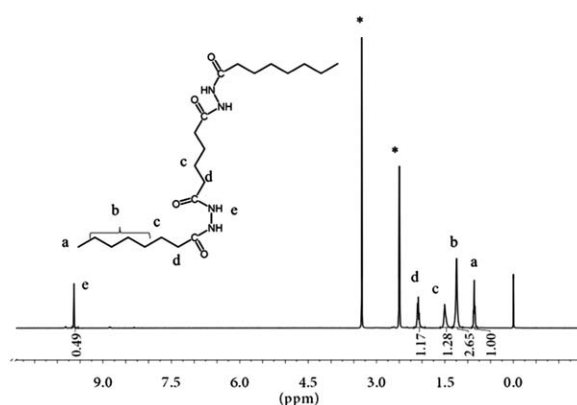


Figure 2. ¹H NMR spectra of ADH-Oc [Asterisks denote the peak ascribed to DMSO and H₂O].

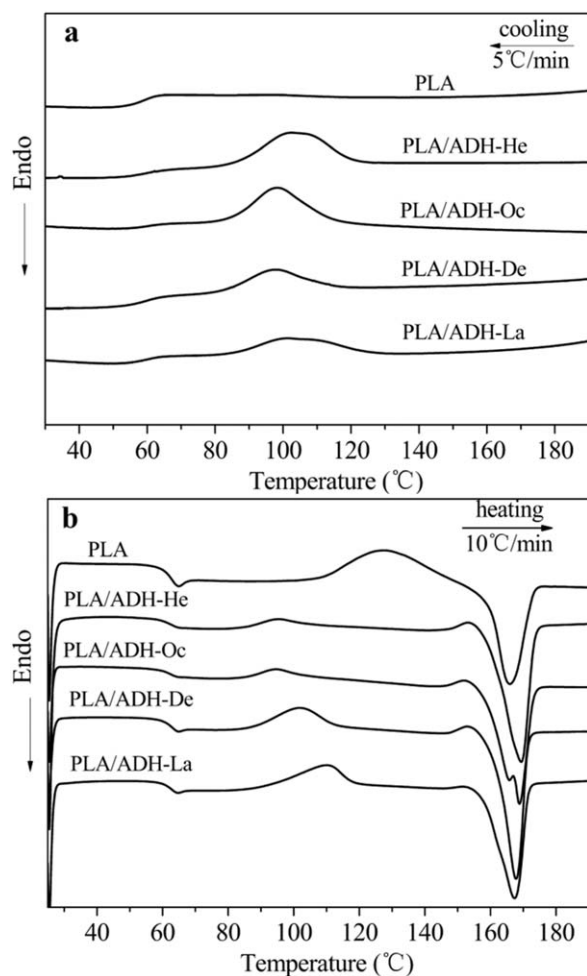


Figure 3. DSC curves of neat PLA and PLA/ADHs: (a) nonisothermal crystallization at a cooling rate of 5°C/min and (b) subsequent heating scan at a rate of 10°C/min.

Preparation of Samples

PLA/ADHs blends were prepared by solution casting method. One g PLA was firstly dissolved in 30 mL dichloromethane and then 1 wt % ADHs were added into the solution. The suspensions were stirred and dispersed with ultrasound for 5 min so that the ADHs particles could disperse in PLA solution uniformly. At last, the blends were casted on glass petri dishes. Then the prepared films were kept in a vacuum oven at 80°C for 12 hours.

Crystallization Behavior

The nonisothermal and isothermal crystallization behaviors of neat PLA and PLA/ADHs were researched by a DSC instrument (Mettler-Toledo, TGA/DSC 1, Switzerland). The measurements were conducted under nitrogen atmosphere. In the nonisothermal crystallization process, about 5–10 mg samples were firstly heated to 200°C at a rate of 30°C/min and hold for 3 min to eliminate thermal history. Then the samples were cooled to 25°C at a decreasing rate of 5°C/min, and were subsequently heated to 200°C at an increasing rate of 10°C/min. Melt crystallization temperature (T_{mc}) and melt crystallization enthalpy (ΔH_{mc}) were obtained during the cooling process, cold crystallization temperature (T_{cc}), cold crystallization enthalpy (ΔH_{cc}), melting temperature (T_m), and melting enthalpy (ΔH_m) were measured during the subsequent heating process. The degree of crystallinity (X_c) values of neat PLA and PLA/ADHs blends were evaluated by the following equation:^{29,30}

$$X_c = \frac{\Delta H_m - \Delta H_{cc}}{\Delta H_m^\infty} \times \frac{1}{\omega} \quad (1)$$

where ΔH_m and ΔH_{cc} are the melting enthalpy and cold crystallization enthalpy in the second heating process, ω is the weight fraction of PLA in the PLA/ADHs blends, and ΔH_m^∞ , which is the melting enthalpy of an infinitely large crystal, was taken as 93.6 J/g.³¹

During the isothermal crystallization process, the samples were also held at 200°C for 3 min to eliminate the thermal history and the blends were then quenched to a desired crystallization temperature with a decreasing rate of 100°C/min. The isothermal test was measured for 20 min and the time dependent crystallization enthalpy (ΔH_c) was automatically recorded by the instrument.

Wide-Angle X-ray Diffraction

PLA and PLA/ADHs blends were isothermal crystallization treated before examined in the wide-angle X-ray diffraction (WAXD) system. WAXD patterns were performed on a D8 Advance diffractometer (Bruker AX, Germany) with a $Cu K_\alpha$ radiation ($\lambda_x = 0.154$ nm). The equipment was operated at 40 kV and 40 mA under ambient temperature. Samples were scanned in fixed time mode with 7 min under diffraction angle 2θ in the range of 5–40°.

Optical Morphology

The PLA spherulites formation and size of the spherulites were observed by a polarized optical microscope (POM, Olympus BX51). The temperature control of these samples was performed using a hotstage (Linkam LTS420). The solution casting films sandwiched between two glass slides were held at 200°C for 3

Table I. Nonisothermal Crystallization Data of Neat PLA and PLA/1 wt % ADHs

Sample	T_{mc} (°C)	ΔH_{mc} (J/g)	T_{cc} (°C)	ΔH_{cc} (J/g)	T_m (°C)	ΔH_m (J/g)	X_c %
PLA	-	-	130	24.1	167	25.4	1.4
PLA/ADH-He	105	20.5	96	2.8	168	28.7	28.0
PLA/ADH-Oc	98	20.3	95	2.6	168	30.4	30.0
PLA/ADH-De	97	11.6	102	8.3	167	27.3	20.5
PLA/ADH-La	103	10.7	110	10.2	167	27.6	18.8

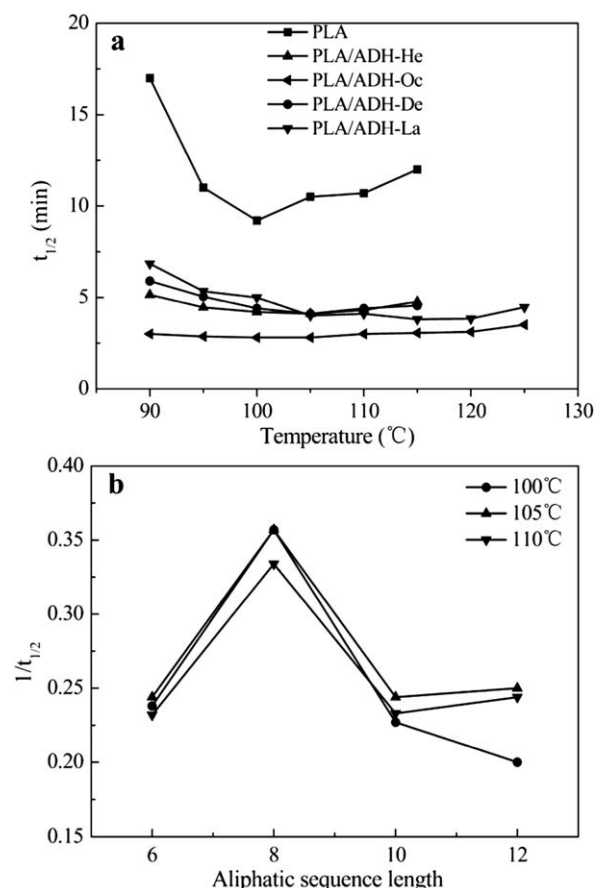


Figure 4. Effect of varying (a) the T_c on the $t_{1/2}$ values of neat PLA and the PLA/ADHs and (b) the rate of crystallization versus aliphatic sequence length at constant T_c .

min and followingly quenched to desired temperature for isothermal crystallization.

RESULTS AND DISCUSSION

Nonisothermal Crystallization

The DSC thermograms of the nonisothermal crystallization for neat PLA and PLA/ADHs blends were all shown in Figure 3. No crystallization peak was detected for neat PLA during the cooling process in Figure 3(a), and a wide cold crystallization peak was observed around 131°C in the subsequent heating process as shown in Figure 3(b). The results illustrated that the crystallization ability of neat PLA was poor and very difficult

to reach high crystallinity during the common nonisothermal crystallization treatment. However, after adding only 1 wt % ADHs, obvious crystallization peak could be detected in the crystallization exotherm of PLA/ADHs blends, indicating that ADHs could enhance the crystallization ability of PLA. Furthermore, the presence of ADHs had an effect on the cold crystallization temperature (T_{cc}) of PLA during subsequently heating process, which led to lower cold crystallization temperatures (T_{cc}). The adding of ADHs did not affect the T_g and T_m of PLA, but the melt crystallization enthalpy (ΔH_{mc}) increased in the PLA/ADHs blends when compared to neat PLA as shown in Table I.

With the addition of 1 wt % ADH-De or ADH-La, small and broad melt crystallization peaks appeared in the cooling scan curves in Figure 3(a), and strong cold crystallization peaks still existed in the subsequent heating process as shown in Figure 3(b). Such results mean that the nucleation effect of ADH-De and ADH-La was very limited. In contrast, by using ADH-He or ADH-Oc, the melt crystallization peaks were much sharper and larger as reflected by ΔH_{mc} and crystallinity in Table I. The cold crystallization peaks almost disappeared in the following heating scan in Figure 3(b), indicating that the crystallization of the PLA was significantly improved in the cooling process. What is more, T_{cc} of PLA/ADH-Oc and PLA/ADH-He decreased to 95°C and 96°C , respectively, which means that the cold crystallization was also elevated. The thermal parameters of PLA and PLA/ADHs blends from nonisothermal crystallization process were listed in Table I. It was found that the crystallinity (X_c) of PLA increased from 1.4% to 30.0% with the addition of 1 wt % ADH-Oc, and the PLA/ADH-Oc blend exhibited the sharpest and narrowest melt crystallization peak in the cooling scan Figure 3(a). Therefore, ADH-Oc was the most efficient nucleating agent for PLA among ADHs. In terms of lower T_{cc} and higher ΔH_{mc} , the nucleation effects decreased in the order of ADH-Oc > ADH-He > ADH-De > ADH-La.

Isothermal Crystallization

PLA and the PLA/ADHs blends were studied by isothermal crystallization at different temperatures. Figure 4(a) showed the crystallization half-time ($t_{1/2}$) of the samples at varying T_c . The crystallization half-time ($t_{1/2}$) was defined as the time achieving 50% of the final crystallinity of the samples. It was noted that the $t_{1/2}$ values of PLA/ADHs were all lower than that of neat PLA. In samples of PLA/ADH-He, PLA/ADH-Oc

Table II. The Avrami Parameters and Thermal Data of Neat PLA and PLA/ADHs Melt Crystallized Isothermally at 100°C , 105°C , and 110°C

Sample	100°C			105°C			110°C		
	$t_{1/2}$ (min)	n	ΔH_c	$t_{1/2}$ (min)	n	ΔH_c	$t_{1/2}$ (min)	n	ΔH_c
PLA	9.2	3.98	26.6	10.7	3.48	27.5	10.5	3.94	24.6
PLA/ADH-He	4.2	5.20	28.7	4.1	4.48	29.5	4.3	5.23	29.2
PLA/ADH-Oc	2.8	3.97	32.1	2.8	4.98	32.9	3.0	4.81	28.4
PLA/ADH-De	4.4	4.81	27.3	4.1	4.25	27.1	4.4	4.05	32.3
PLA/ADH-La	5.0	3.91	31.3	4.0	3.06	35.0	4.1	3.14	33.1

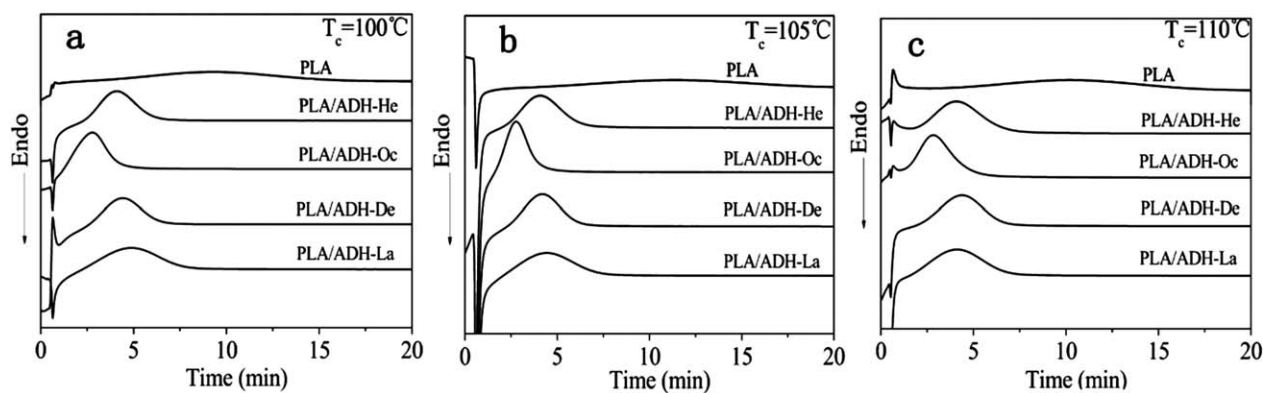


Figure 5. DSC curves of isothermal crystallization of neat PLA and PLA/ADHs at (a) 100°C, (b) 105°C, and (c) 110°C.

and PLA/ADH-De, the minimum of $t_{1/2}$ appeared at 105°C. But in sample PLA/ADH-La, the shortest $t_{1/2}$ located between 115°C and 120°C, and below 115°C $t_{1/2}$ increased as temperature decreased. It was interesting to note the temperature difference of minimum $t_{1/2}$ among these systems, and such results could be attributed to crystalline structure, particle size, distribution etc. As shown in Table II, the $t_{1/2}$ of PLA/ADH-He, PLA/ADH-De, and PLA/La was about 4 min from 100°C to 110°C, and the shortest $t_{1/2}$ was 2.8 min for PLA/ADH-Oc at 105°C. Crystallization rate at constant T_c can be inversely reflected by crystallization half-time ($t_{1/2}$) as shown in Figure 4(b). It was clearly shown that growth of PLA crystallites is the fastest when ADH-Oc is present. It showed that ADH-Oc was the most effective nucleating agent among these compounds, because $t_{1/2}$ in PLA/ADH-Oc was always lower than

others and the crystallinity was higher than others in the experimental temperature region. It may be interpreted by the fact that PLA chains could attach well to the surface of the ADH-Oc nucleus.

The isothermal crystallization for neat PLA and PLA/ADHs blends at 100°C, 105°C, and 110°C were showed in Figure 5 as examples. As can be seen from Figure 5, the heat flow of neat PLA changed very slowly, and no sharp crystallization peaks could be found during the isothermal process. In contrast, for all the PLA/ADHs blends, obvious and sharp crystallization peaks could be observed. As can be seen from Table II, the crystallization enthalpy (ΔH_c) of PLA could reach high values after the isothermal crystallization for 20 min, but the ΔH_c of blends could reach its maximum value in a much shorter time. This

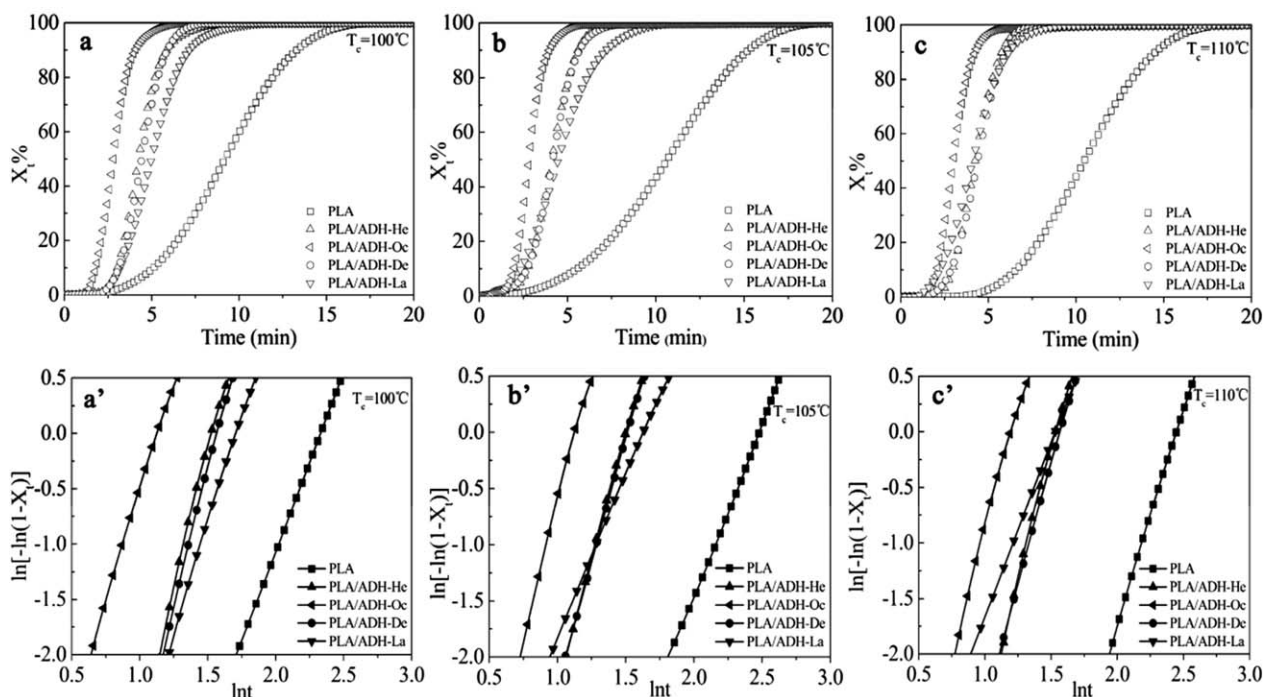


Figure 6. The relative crystallization (X_t) as a function of crystallization time (a, b, c) and Avrami plots of neat PLA and PLA/ADHs isothermal crystallization at different temperatures (a', b', c').

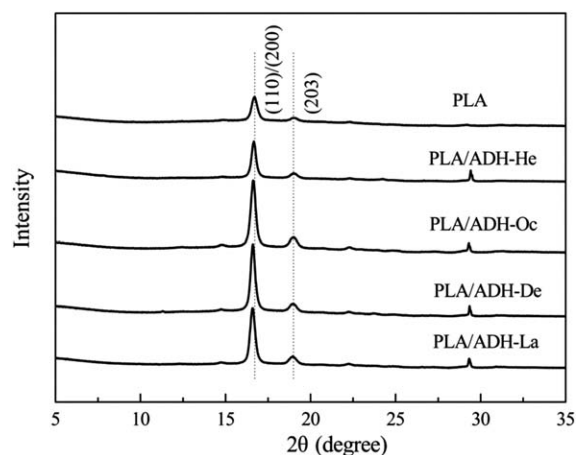


Figure 7. WAXD patterns of neat PLA and PLA/ADHs treated by isothermal crystallization at 105°C for 5 min.

result again affirmed that the addition of ADHs could improve the crystallization rate of PLA.

The isothermal crystallization could be described by the well-known Avrami equation.^{32–34} In this equation, relative crystallinity X_t was defined as in the following equation:

$$1 - X_t = \exp(-kt^n) \quad (2)$$

where n is the Avrami exponent and k is the rate constant of crystallization. Usually, the Avrami exponent n depends on the mechanism of nucleation and the type of crystal growth.³⁵

Equation (2) can be rearranged into linear form as given by Equation:

$$\ln[-\ln(1 - X_t)] = \ln k + n \ln t \quad (3)$$

Then the parameter n can be obtained from the slope of plot of $\ln[-\ln(1 - X_t)]$ versus $\ln t$, and the intercept is $\ln k$.

Figure 6 showed the curves of X_t versus crystallization time in the row above and the plots of $\ln[-\ln(1 - X_t)]$ versus $\ln t$ for the neat PLA and PLA/ADHs blends in the row below. As shown in Figure 6, linear fit well described the Avrami equation for all the samples. The Avrami exponent n was calculated by employing Avrami equation and listed in Table II. It could be found that the Avrami exponent n differed from sample to sample, and it also varied with T_c . For neat PLA, the values of n were around 4, reflecting homogeneous nucleation with a three-dimensional crystal growth.³⁶ In contrast, most of n values of the PLA/ADHs blends were between 3 and 5 and no regular law can be found in these samples, which may be explained by the complicated competition between grain boundaries, chemical group compatibilities and lattice match, etc.³⁷ Since n depends on many factors, such as the nucleation density, blending, crystalline type, and restriction of crystalline formation, it needs further investigation in the future.

Wide-Angle X-ray Diffraction

The WAXD patterns of neat PLA and PLA/ADHs blends, treated by the process of isothermal melt crystallization at 105°C for 5 min, were shown in Figure 7. Neat PLA showed two weak diffraction peaks ($2\theta = 16.90^\circ$, $2\theta = 19.15^\circ$). It can

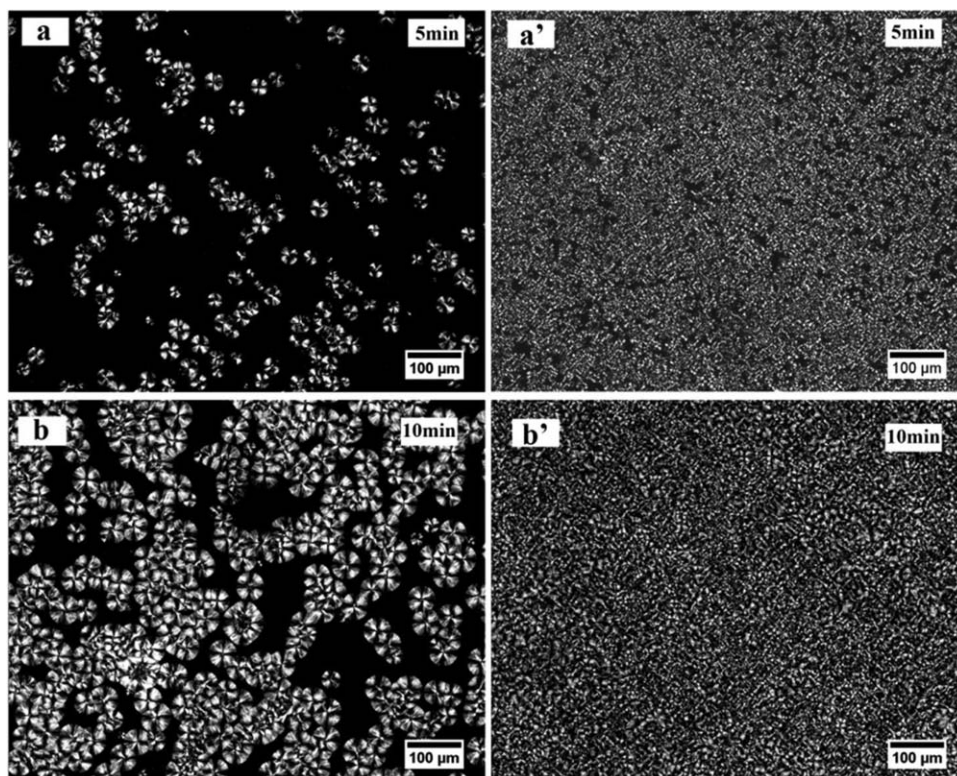


Figure 8. POM images of neat PLA (a, b) and PLA/ADH-Oc (a', b') crystallized isothermally at 120°C for 5 min and 10 min.

be attributed to the crystals of neat PLA. While PLA/ADHs blends exhibited a strong diffraction peak at 16.89° and a weak peak at 18.99° , which related to the (200)/(110) and (203) planes, respectively, and were the characteristic peaks of PLA crystallite.³⁸ Another weak peaks were observed at 29.3° , which were the diffraction of ADHs crystals. The results indicated that the crystallinity of PLA was improved while the crystalline structure was not discernibly affected by the addition of ADHs.

Optical Morphology

Based on the findings above, ADH-Oc was selected as a typical effective nucleating agent for further analysis to evaluate its nucleation ability. The spherulite morphology of neat PLA and PLA/ADH-Oc were analyzed under a polarized optical microscope. We selected a high crystallization temperature (120°C) to distinguish homogeneous nucleation and heterogeneous nucleation in the samples and monitor the morphology in the course of crystallization. As shown in Figure 8, it was obvious that the size of spherulites in PLA were much bigger than those in the PLA/ADH-Oc blends crystallized isothermally at 120°C for 5 and 10 min. Moreover, the number of growing spherulites ascended with time in neat PLA, whereas the number of growing crystallites seemed stay almost constant in PLA/ADH-Oc. This result showed that ADH-Oc could provide more nucleation sites for the crystallization and heterogeneous nucleation dominated in PLA matrix. With increased nucleation, the crystallization ability of PLA was enhanced greatly, which was consistent with the previous results.

CONCLUSIONS

Four different aliphatic diacyl adipic dihydrazides (ADHs) were synthesized and investigated as the nucleating agents for PLA. The results of nonisothermal and isothermal crystallization results showed that ADHs could enhance the crystallinity, gave high ΔH_{mc} and lowered the cold crystallization (T_{cc}) of PLA. Among them, ADH-Oc was the most effective nucleating agent in terms of fastest crystallization rate and highest crystallinity. The blend of PLA/ADH-Oc exhibited a very short crystallization half-time around 2.8 min at 105°C . In addition, WAXD analysis revealed that ADHs could improve the crystallization of PLA but has no effect on the crystalline structure. POM investigation showed that the PLA with the addition of ADH-Oc could form smaller spherulites and larger nucleation density. Thus, this study suggested ADH-Oc is simple and potential nucleating agent to enhance crystallization ability of PLA.

ACKNOWLEDGMENTS

We greatly thank the financial support from the NSFC projects (No. 21204096, No. 21274160) and Ningbo Key Lab of Polymer Materials (grant No. 2010A22001).

REFERENCES

1. Chandra, R.; Rustgi, R. *Prog. Polym. Sci.* **1998**, *23*, 1273.
2. Babu, R.; O'Connor, K.; Seeram, R. *Prog. Biomater.* **2013**, *2*, 1.
3. Ikada, Y.; Tsuji, H. *Macromol. Rapid. Commun.* **2000**, *21*, 117.
4. Kim, K.; Yu, M.; Zong, X.; Chiu, J.; Fang, D.; Seo, Y. S.; Hsiao, B. S.; Chu, B.; Hadjiargyrou, M. *Biomaterials* **2003**, *24*, 4977.
5. Auras, R.; Harte, B.; Selke, S. *Macromol. Biosci.* **2004**, *4*, 835.
6. Seppälä, J. V.; Helminen, A. O.; Korhonen, H. *Macromol. Biosci.* **2004**, *4*, 208.
7. Sinclair, R. J. *Macromol. Sci. A Pure. Appl. Chem.* **1996**, *33*, 585.
8. Lim, L. T.; Auras, R.; Rubino, M. *Prog. Polym. Sci.* **2008**, *33*, 820.
9. Sajjad Saeidlou, M. A. H. *Prog. Polym. Sci.* **2012**, *37*, 1657.
10. Barrau, S.; Vanmansart, C.; Moreau, M.; Addad, A.; Stoclet, G.; Lefebvre, J. M.; Seguela, R. *Macromolecules* **2011**, *44*, 6496.
11. Liao, R. G.; Yang, B.; Yu, W.; Zhou, C. X. *J. Appl. Polym. Sci.* **2007**, *104*, 310.
12. Harris, A. M.; Lee, E. C. *J. Appl. Polym. Sci.* **2008**, *107*, 2246.
13. Tsuji, H.; Takai, H.; Saha, S. K. *Polymer* **2006**, *47*, 3826.
14. Li, H.; Huneault, M. A. *Polymer* **2007**, *48*, 6855.
15. Hassouna, F.; Raquez, J. M.; Addiego, F.; Dubois, P.; Toniazzi, V.; Ruch, D. *Eur. Polym. J.* **2011**, *47*, 2134.
16. Hassouna, F.; Raquez, J. M.; Addiego, F.; Toniazzi, V.; Dubois, P.; Ruch, D. *Eur. Polym. J.* **2012**, *48*, 404.
17. Hu, Y.; Hu, Y. S.; Topolkarayev, V.; Hiltner, A.; Baer, E. *Polymer* **2003**, *44*, 5681.
18. Tabi, T.; Sajo, I.; Szabo, F.; Luyt, A.; Kovacs, J. *Express. Polym. Lett.* **2010**, *4*, 659.
19. Carrasco, F.; Pages, P.; Gamez-Perez, J.; Santana, O. O.; MasPOCH, M. L. *Polym. Degrad. Stabil.* **2010**, *95*, 116.
20. Yu, F.; Liu, T.; Zhao, X.; Yu, X.; Lu, A.; Wang, J. *J. Appl. Polym. Sci.* **2012**, *125*, E99.
21. Tsuji, H.; Takai, H.; Fukuda, N.; Takikawa, H. *Macromol. Mater. Eng.* **2006**, *291*, 325.
22. Battagazzore, D.; Bocchini, S.; Frache, A. *Express. Polym. Lett.* **2011**, *5*, 849.
23. Jimenez, G.; Ogata, N.; Kawai, H.; Ogihara, T. *J. Appl. Polym. Sci.* **1997**, *64*, 2211.
24. Nam, J. Y.; Okamoto, M.; Okamoto, H.; Nakano, M.; Usuki, A.; Matsuda, M. *Polymer* **2006**, *47*, 1340.
25. Xing, Q.; Zhang, X.; Dong, X.; Liu, G.; Wang, D. *Polymer* **2012**, *53*, 2306.
26. Cai, Y. H.; Yan, S. F.; Fan, Y. Q.; Yu, Z. Y.; Chen, X. S.; Yin, J. B. *Iran. Polym. J.* **2012**, *21*, 435.
27. Kawamoto, N.; Sakai, A.; Horikoshi, T.; Urushihara, T.; Tobita, E. *J. Appl. Polym. Sci.* **2007**, *103*, 198.
28. Kawamoto, N.; Sakai, A.; Horikoshi, T.; Urushihara, T.; Tobita, E. *J. Appl. Polym. Sci.* **2007**, *103*, 244.
29. Vasanthakumari, R.; Pennings, A. *J. Polymer* **1983**, *24*, 175.

30. Reinsch, V. E.; Kelley, S. S. *J. Appl. Polym. Sci.* **1997**, *64*, 1785.
31. Tang, Z.; Zhang, C.; Liu, X.; Zhu, J. *J. Appl. Polym. Sci.* **2012**, *125*, 1108.
32. Avrami, M. *J. Chem. Phys.* **1939**, *7*, 1103.
33. Avrami, M. *J. Chem. Phys.* **1940**, *8*, 212.
34. Avrami, M. *J. Chem. Phys.* **1941**, *9*, 177.
35. Qiu, Z.; Li, Z. *Ind. Eng. Chem. Res.* **2011**, *50*, 12299.
36. Miyata, T.; Masuko, T. *Polymer* **1998**, *39*, 5515.
37. Battegazzore, D.; Bocchini, S.; Frache, A. *Express. Polym. Lett.* **2011**, *5*, 849.
38. Pan, P.; Kai, W.; Zhu, B.; Dong, T.; Inoue, Y. *Macromolecules* **2007**, *40*, 6898.